

# The Manufacture of Fancy Laces by Machine

By FRITZ KEUNECKE, BARMEN, GER.

*(Continued from January issue, page 1502)*

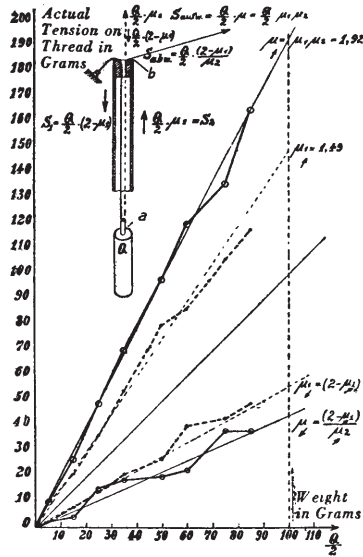
## IV. The Influence of Friction on Thread Tension

### (a) Principle

The thread friction in a carrier is composed of: friction in the guide eyelet of the thread tension device caused by the up and down movement, and friction in the upper guide eyelet of the carrier proper. Figure 15 shows the scheme of the thread guide. We presume that the left end of the yarn coming from the bobbin is fastened, since in actual

practice the bobbin is usually locked by a brake lever. The thread is now carried downward in the carrier pipe through the eyelet of weight  $Q$ , then goes upward through the fixed carrier eyelet  $b$  and from there it goes at an angle of from  $12^\circ$  to  $15^\circ$  diagonally upward to the braiding point of the machine. In practical usage the eyelet  $a$  is usually formed from steel wire of 1.5 to 2.5 mm. diameter, the eyelet  $b$ , however, ordinarily consists of a glazed china ring. In both eyelets the thread is subject to friction, depend-

ing in its intensity upon the weight  $Q$ , the smoothness or roughness of the thread or of the eyelets, the angle of the loop, and finally the speed of the machine.



Figs. 15 & 16

Assuming the lettering  $S_1$  and  $S_2$  for the two thread pendants enclosed in the carrier pipe, both pendants have the same tension in rest position or:

$$S_1 = S_2 = \frac{Q}{2} \quad (6)$$

During the movement of the carrier there occurs continuously a pulling up and letting down of the right thread pendant. During the pulling up period of the thread,  $S_2$  will become larger than  $S_1$ , or according to the formula of rope friction:

$$S_2 = S_1 \cdot e^{\mu' a} \quad (7)$$

where the letter  $\mu$  stands for the specific friction between two raw materials (in this instance *yarn* vs. *steel*). Since the loop angle at eyelet  $a$  remains  $a$  constant  $= \pi$  and since we are trying to find the influence of the weight  $Q$  upon the thread tension, we may state the formula:

$$S_2 = \frac{Q}{2} \cdot \mu_1 \quad (8)$$

where  $\mu_1$  represents the factor for the increase of thread tension caused by friction in eyelet  $a$  in contrast to the average value caused by the weight  $Q$ .

In the other thread pendant, the left one, friction is diminished in the same proportion, and since  $S_1 + S_2 = Q$ , we receive:

$$S_1 = \frac{Q}{2} \cdot (2 - \mu_1) \quad (9)$$

Both equations (8) and (9) are only correct for the *upward* movement of the thread tension device, or for the moving of the carrier *away* from the braiding point. During the contrary movement of the carrier the tension shows the opposite tendency, consequently the formulas for the *downward* movement of the thread tension device are:

$$S_1 = \frac{Q}{2} \cdot \mu_1 \quad (10)$$

$$S_2 = \frac{Q}{2} \cdot (2 - \mu_1) \quad (11)$$

Furthermore the thread tension is influenced by the friction in the upper eyelet  $b$ . Let us set for this friction the factor  $\mu_2$ , so the resulting force attacking at this point of the thread will be expressed:

$$S \text{ Upward} = \frac{Q}{2} \cdot \mu_1 \cdot \mu_2 \quad (12)$$

$$S \text{ Downward} = \frac{Q}{2} \cdot \frac{2 - \mu_1}{\mu_2} \quad (13)$$

### (b) Measuring Thread Friction at the Carrier

To find actual values for the factors  $\mu_1$  and  $\mu_2$  of the friction element, a spring-scale was hooked to the free end of the thread and thus the friction causing thread tension during the pulling up and letting down of the yarn could be measured. (See Figure 17). These readings were carried out with different weights, and upwards as well as downwards, in strictly vertical direction of the scale to find the value for  $\mu_1$  or  $(2 - \mu_1)$  and also in diagonal direction of the scale approximately to  $S$  and thus finding the value of  $\mu_1 \cdot \mu_2$  and  $\frac{2 - \mu_1}{\mu_2}$  respectively.

The results of these measurements are given in graphic curves (Figure 16) and the numerical findings are also computed (Figure 17). The points of the two lower curves show slight irregularities; first, within the limits the

Load in Grams		↑		↓		↗		↘					
		Tension Vertically Upward p in grams		Tension Vertically Down p in grams		Angular Tension Upward p in grams		Angular Tension Downward p in grams					
G	G/2	R'dg.	Corrected R'dg.	$\mu = \frac{G}{2}$	R'dg.	Corrected R'dg.	$\mu = \frac{G}{2}$	R'dg.	Corrected R'dg.	$\mu = \frac{G}{2}$	R'dg.	Corrected R'dg.	$\mu = \frac{G}{2}$
10	5	10	10		2	2		10	10	10	2	2	
20	10	16	16	1.6	4	4	0.48	18	19	1.9	3	3	0.3
30	15	20	21	1.4	8	8	0.56	25	27	1.8	4	4	0.26
40	20	30	32	1.6	12	12	0.6	35	38	1.9	7	7	0.36
50	25	35	37	1.48	13	14	0.56	45	49	1.96	14	15	0.78
70	35	50	54	1.52	19	21	0.6	65	70	2.0	18	19	0.54
90	45	65	70	1.54	25	27	0.6	80	84	1.88	19	20	0.44
100	50	75	80	1.6	25	27	0.54	95	98	1.96	19	20	0.4
120	60	82	86	1.44	37	40	0.66	120	121	2.0	22	23	0.38
150	75	105	106	1.42	40	43	0.56	135	136	1.82	35	38	0.5
170	85	115	116	1.36	45	49	0.58	165	165	1.94	25	38	0.44
		Average		1.49	Average		.56	Average		1.92	Average		.44

readings of the spring-scale became inaccurate; second, the changing consistency of the thread strongly influenced the values at these low tensions.

The experiments were carried out with regular medium cotton yarn (12/3), the lower eyelet *a* was 1.5 mm. spring steel, as cus-

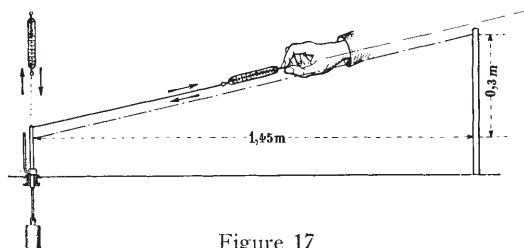


Figure 17

tomary for one thread lace machines of this type. The upper eyelet *b* was a glazed china ring of the same consistency as all other carrier eyelets of the experimental lace machine. The spring-scale was thoroughly tested before the experiment and all readings were corrected according to the gauge standard. It is clearly evident from the graphic curves that at both points of friction or for both directions of movement *the thread friction is in direct proportion to the loading*. Furthermore the experiments show that the friction of rest is no more than the friction during movement.

This movement (the speed of pulling or releasing the thread with the spring-scale) averaged 5 cm. (= ca 2 inch) per second.

The motion was caused by hand, which moved the spring-scale slowly from rest position. The tension of the scale at first accelerated to a point at which the thread followed and started sliding. There was no change in tension value compared with the highest rest position tension. When the speed of the thread pulling was increased, a slight increase in tension was noticeable. These experiments, however, did not show conclusively, if and how a change was caused by acceleration of the tension weight used as load. To find additional facts about the relationship between the amount of friction and speed, a number of experiments were required, which will be described in the next chapter.

The experiment previously described clearly proved that with the quality of yarn tested during the pulling-out period of the thread (when the carrier moves *away from the braiding point*), the thread tension shows *about twice the value of the average tension*; while the *actual tension drops to about half of the average tension* as soon as the carrier *approaches the braiding point*.

### (c) General Determination of Yarn Friction in Relation to Braiding Speed

Since one-thread laces are mostly manufactured from soft, smooth, pliable yarn the internal friction of the thread may be considered as negligible. According to the formula for

rope friction there exists between the tractive forces of both thread pendants (see equation 7) the relationship:

$$S_2 = S_1 \cdot e^{\mu' \alpha} \quad (14)$$

or

$$\frac{S_2}{S_1} = e^{\mu' \alpha} \quad (15)$$

W. Krumme, Barmen, Ger., recommended the following arrangement (see Figure 18)

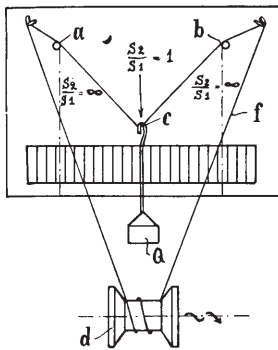


Figure 18

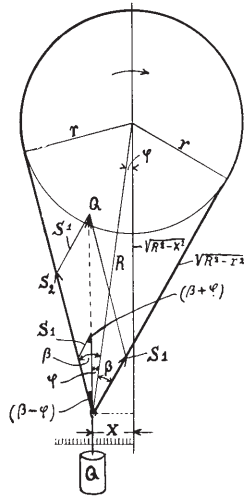


Figure 19

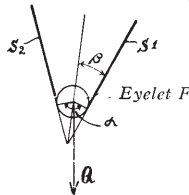


Figure 20

for finding the friction factor  $\mu'$  in its dependency upon speed. According to this lay-out the yarn to be tested is led as an endless thread  $f$  over fixed guiding points  $a$  and  $b$ , and between these guiding points the eyelet  $c$ , loaded with weight  $Q$ , is hooked to the thread. The thread  $f$  is driven by a roller  $d$ . Under the influence of tension weight  $Q$  the thread part fixed between the points  $a$  and  $b$  forms an isosceles triangle, as long as the thread does not move. As soon as the thread is set in motion the point  $c$  of the triangle (according to the direction of the movement) shifts in an elliptic curve to the right or to the left until a new state of balance has been found. The swinging of the pendulum is a standard of measurement for the difference in tension  $S_1/S_2$ . It may be read from a scale.

## Principle of the Experimental Arrangement

The proposition described above has been used as the basis of the experiments. To obtain a more simplified mathematical relation the arrangement of Krumme has been changed, in that a single large idler pulley has been adopted which serves at the same time as driving device. (See Figure 19.)

The experimental rigging finally used in our experiments is shown in Figure 21. The pulley  $g$  is arranged so that it may be driven at variable speeds. The thread eyelet moves sideward for a certain distance  $x$ , which may be read off from scale  $h$ . This arrangement has the advantages that the length of both thread pendants and the loop angle formed by the eyelet remain the same. The scale reading  $x$ , after previous correction, immediately shows the friction factor  $\mu'$ .

## Mathematical Relationship Between $\mu'$ and Scale Reading $x$ of the Experiment

The mathematical relations between  $x$  and  $\mu'$  according to Figures 19 and 20 may be deducted as follows:

When pulley  $g$  is turned in the direction of the arrow, the weight  $Q$  moves to the left for the distance  $x$  until equilibrium of forces is established. In the triangle of forces drawn the sine relation will show:

$$\frac{S_2}{S_1} = \frac{\sin(\beta + \varphi)}{\sin(\beta - \varphi)} \quad (16)$$

according to equation (15) we found:

$$\frac{S_2}{S_1} = e^{\mu' a} = \frac{\sin(\beta + \varphi)}{\sin(\beta - \varphi)}$$

consequently for  $\mu' = \frac{1}{\alpha} \cdot \ln \frac{\sin(\beta + \varphi)}{\sin(\beta - \varphi)}$

whereby  $a = \frac{1}{\alpha} \cdot \ln \frac{\sin \beta \cos \varphi + \cos \beta \sin \varphi}{\sin \beta \cos \varphi - \cos \beta \sin \varphi}$

is the angle of the eyelet suspension point, which amounts to  $120^\circ$  in the experiment. If we replace the functions of the angles by the corresponding distances (see Figure 19) we have:

$$\mu = \frac{1}{\alpha} \cdot \ln \frac{\frac{r}{R} \cdot \frac{\sqrt{R^2 - x^2}}{R} + \frac{x}{R} \cdot \frac{\sqrt{R^2 - r^2}}{R}}{\frac{r}{R} \cdot \frac{\sqrt{R^2 - x^2}}{R} - \frac{x}{R} \cdot \frac{\sqrt{R^2 - r^2}}{R}}$$

$$\mu = \frac{1}{\alpha} \cdot \ln \frac{r \sqrt{R^2 - x^2} + x \sqrt{R^2 - r^2}}{r \sqrt{R^2 - x^2} - x \sqrt{R^2 - r^2}} \quad (17)$$

In this formula the values  $a$ ,  $r$ ,  $R$ , are constant or may be kept constant, and at different speeds, only  $x$  is changeable, by which we may arrive at the corresponding friction value  $\mu_1$ . Assuming that  $r$ , and consequently  $x$ , in relation to  $R$  are only small, the equation (17) may be changed to a more simplified form. If we divide by  $R$  the numerator and the denominator of the fraction we have accordingly:

$$\frac{r \sqrt{1 - \frac{x^2}{R^2}} + x \sqrt{1 - \frac{r^2}{R^2}}}{r \sqrt{1 - \frac{x^2}{R^2}} - x \sqrt{1 - \frac{r^2}{R^2}}}$$

Here we may replace each of the root values by the beginning of a binomial series, as follows:

$$\frac{r \left[ 1 - \frac{1x^2}{2R^2} - \frac{1}{8} \left( \frac{x^2}{R^2} \right)^2 \dots \right] + x \left[ 1 - \frac{1r^2}{2R^2} - \frac{1}{8} \left( \frac{r^2}{R^2} \right)^2 \dots \right]}{r \left[ 1 - \frac{1x^2}{2R^2} - \frac{1}{8} \left( \frac{x^2}{R^2} \right)^2 \dots \right] - x \left[ 1 - \frac{1r^2}{2R^2} - \frac{1}{8} \left( \frac{r^2}{R^2} \right)^2 \dots \right]}$$

We choose for instance,  $r/R = 1/5$ , so we receive for the second term  $1/2 \cdot r^2/R^2$  the value  $1/50$  and for the third term only  $1/5000$ . Since  $x$  is always smaller than  $r$ , (in practical experiments about  $r/2$ ) we find in the first bracket that the second and third terms become still smaller and amount to only  $1/4$  of the corresponding terms of the second bracket. Based upon the experimental arrangement of  $r/R = 1/5$ , it appears accurate enough for the numerator as well as for the denominator to consider in the first bracket the first term only, and in the second bracket the first and second terms only. The fraction thus appears much more simplified:

$$\frac{r + x \left( 1 - \frac{r^2}{R^2} \right)}{r - x \left( 1 - \frac{r^2}{R^2} \right)}$$

$$R = 307 \text{ mm}; r = 167 \text{ mm}, x = 2$$

mm	0	10	20	30	40	50	60	70	80
$\mu'$	0	0.035	0.078	0.124	0.177	0.235	0.308	0.381	0.453

In practical usage the arrangement  $r/R = 1/5$  permits the dropping of the second term of the bracket as negligible; then we receive instead of equation (17) the simplified relation:

$$\mu' = \frac{1}{\alpha} \ln \frac{r+x}{r-x} \quad (17a)$$

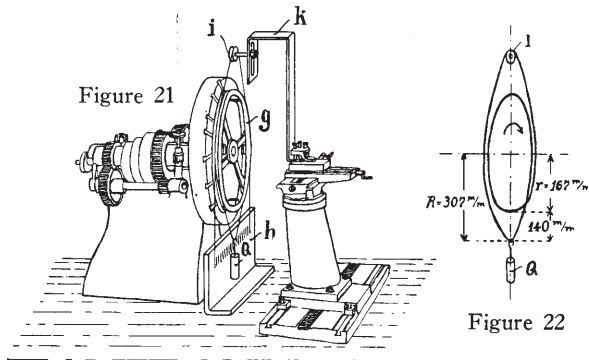
## Experimental Procedure

As can be seen from Figure 21 a pulley having a radius of 167 mm was driven at different speeds on a lathe frame. Below the disc was mounted a scale  $h$ , and the thread suspended from disc  $g$  was loaded with a tension weight  $Q$ . In order to be able to regulate the distance of the thread eyelet from the pulley axis, one endpiece of the thread was carried over an idler  $i$  suspended over pulley  $g$ . Idler  $i$  was attached to a bracket  $K$ , and could be changed in position relative to the center of the pulley  $g$  by means of a slot. This eliminated the possibility of yarn slipping along the pulley, especially since the thread was carried twice around the circumference in a manner shown in Figure 22. This arrangement offered the advantage that the length of the endless thread was increased and, therefore, the unavoidable knot run through the eyelet only at infrequent intervals. This allowed sufficient time to enable us to obtain correct meter readings.

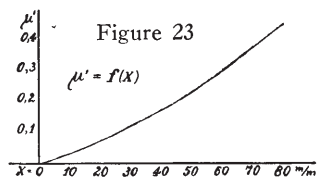
The experimental arrangement of the thread eyelet as to height was chosen so that the eye appears right in front of the scale  $h$  at a distance of  $R = 307$  mm from the center axis of the pulley. At this distance the angle of the thread pendants was  $a = 2$  (in circular measure).

According to equation (17) the following scales of  $x$  and the corresponding values of  $\mu'$  were computed for usage during the experiment. The following table gives their numerical valuation; Figure 23 shows the same as a gauge curve.

The experiments were carried out with different types of carrier eyelets and with different yarns. The thread eyelet was at first a wire loop of 1.5 mm diameter steel wire and then a glass ring of 3 mm diameter. This corresponds in friction effects to the tension spring of the carrier and to the china eye of the carrier proper in actual practice, as illustrated in Figure 15.



The different types of yarn used during the experiment were: 12/3 cotton (the same as in experiment Figure 15), 80/2 luster (cotton) yarn and 300 denier rayon.



This gave a basis of comparison concerning the friction effects on these different materials.

The results are graphically demonstrated in Figure 24 and numerically in the table below.

As evident from Figure 24 in harmony with the findings of figures 15 to 17 the friction of rest is not more than the friction of motion. Furthermore, Figure 24 shows that friction increases with higher speed, at first quickly and then more slowly. At the machine tested, the speed of the thread in the tension eyelet varied between 0 and 0.202 m/sec; in the upper carrier eye the variations, however, had twice the value, i e., between 0 and 0.404 m/sec. The friction factors reach pretty near the upper limit.

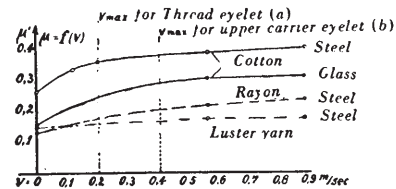


Figure 24

(d) Application of Friction Factor Found in IV c to Carrier Conditions and Comparison with Values Found in IV b

In Figures 15 to 17 we measured the thread tension in a carrier and found the equations

	Adjustment <i>v</i> in m/sec	Reading <i>x</i>	From Gauge Curve $\mu' = f(z)$ Fig. 23
Cotton 12/3 Eyelet: Steel 1.5 mm diam.	0.0	55	0.27
	0.119	65	0.34
	0.2	67	0.355
	0.56	72	0.395
	0.88	74	0.41
Cotton 12/3 Eyelet: Glass 3 mm diam.	0	37	0.16
	0.56	60	0.308
	0.88	61	0.312
Luster (Cotton) Yarn 60/2 Eyelet: Steel 1.5 mm diam.	0	37.5	0.152
	0.56	40	0.177
	0.88	40	0.177
Rayon 300 den. Eyelet: Steel 1.5 mm diam.	0	32	0.135
	0.56	47	0.22
	0.88	51	0.24

(8) and (9) for the upward movement of the thread tension device.

$$S_2 = \frac{Q}{2} \cdot \mu_1$$

$$S_1 = \frac{Q}{2} \cdot (2 - \mu_1)$$

$$\frac{S_2}{S_1} = \frac{\mu_1}{2 - \mu_1}$$

On the other hand according to equation (15) :

$$\frac{S_2}{S_1} = e^{\mu' a}$$

Between the specific friction factor  $\mu'$  and the friction factor  $\mu$  relating only to the tension weight  $Q$  regarding the thread tension eyelet  $a$  there exists a relationship.

$$\frac{\mu_1}{2 - \mu_1} = e^{\mu' a}$$

From this follows the deduction.

$$\mu_1 = \frac{2 \cdot e^{\mu' a}}{1 + e^{\mu' a}} \quad (18)$$

For the thread tension eyelet  $a$  the angle  $a = \pi$ ;  $\mu'$  is according to the curve  $\mu' = f(v)$  to be taken from Figure 24 and the distance  $v = \frac{1}{2} \cdot 0.05$  m/sec., since during the experiment done by hand we pulled the thread from the carrier with a speed of 0.05 m/sec. and the speed at the thread tension eyelet is only half the other speed. At the speed of 0.025 m/sec. accepted for the steel eyelet of 1.5 mm wire diameter we receive, according to curve

below:  $\mu_1 = 1.433$ . We may consider this a good check on the value received according to IV b;  $\mu_1 = 1.49$ .

According to equations (7), (8), and (12) there exists for  $\mu^2$  the relationship

$$S = S_2 \cdot \mu_2$$

$$\text{or } \mu_2 = \frac{S}{S_2} = e^{\mu' a}$$

The angle  $a = 90^\circ - 12^\circ = 78^\circ$ , speed  $v = 0.05$  m/sec. and  $\mu_1$  to be taken from curve, Figure 24, for the thread passing through 3 mm diameter glass ring. Then we have as the result:

$$\mu_2 = e^{\mu' a} \quad (19)$$

$$\mu_2 = e^{0.19 \cdot 1.36} = 1.37$$

The factor of total friction is accordingly:

$$\mu = \mu_1 \cdot \mu_2 = 1.96$$

Here also we find a close check with the value found by hand testing under IV b; the value for  $\mu$  in that case was found to be = 1.92.

In the following tables the values for  $\mu_1$  and  $\mu_2$  according to equations (18) and (19)

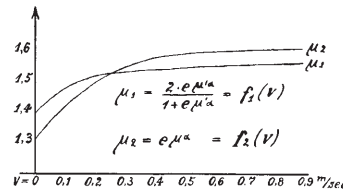


Figure 25

are found for the different speeds of the

$\mu_1 = \frac{2 \cdot e^{\mu' a}}{1 + e^{\mu' a}}$					$\mu_2 = e^{\mu' a}$			
for $a = \pi$ and $\mu'$ from Fig. 24 for Steel eyelet 1.5 mm					for $a = 1.36$ and $\mu'$ from Fig. 24 for Glass eyelet 3 mm			
$v$	$\mu'$	$\mu' a$	$e^{\mu' a}$	$\mu_1$	$v$	$\mu'$	$\mu' a$	$\mu_2$
0	0.27	0.849	2.35	1.4	0	0.16	0.218	1.41
0.119	0.34	1.068	2.91	1.49	0.119	0.225	0.306	1.44
0.2	0.355	1.13	3.1	1.52	0.2	0.255	0.347	1.5
0.56	0.395	1.24	3.5	1.55	0.56	0.308	0.419	1.6
0.88	0.41	1.285	3.65	1.565	0.88	0.312	0.424	1.61
Comparison with hand experiment according to IV b.								
0.025	0.29	0.912	2.53	1.433	0.05	0.19	0.258	1.37

Figure 24, the value  $\mu_1 = 0.29$ . Let us insert these valuations  $a$  and  $\mu_1$  into the equation (18), so we receive as evident from the tables

thread motion. Figure 25 shows the corresponding curves for  $\mu_1$  and  $\mu_2$  as functions of the thread speed.

ure 27 and then take the corresponding value of  $\mu$  from Figure 26. The momentary values of the tension must be multiplied by the corresponding  $\mu$  values, and the result is the strong dot-dash curve drawn in the figure, which presents the theoretical course of the thread tension under consideration of all circumstances entering into the problem.

This treatise is based upon the thread part pending between the braiding point and the carrier, since according to experience this part of the thread undergoes the hardest strain and has the most breakages. A principal characteristic of this curve is a sudden strong increase in tension and a gradual decrease in tension. The sudden tension increase by friction comes in the moment of peak load due to the acceleration force of the weight. Since this force of acceleration increases as  $\omega^2$ , with an increase in revolutions the tension weight carrier has to stand a much more sudden increase in tension; the result is inevitably the breaking of the thread. The weight carrier in this respect is very impractical and causes a strong jerking tension of the thread, even under the normal and customary number of revolutions per minute.

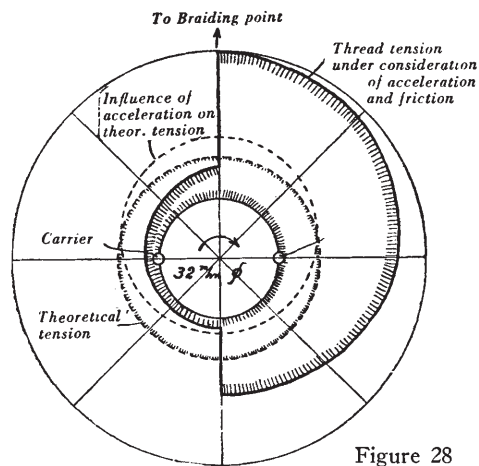


Figure 28

To visualize the course of the thread tension, Figure 28 illustrates the polar coordinates and thus the dependency of thread tension upon the position of the carrier in its course. This sketch shows clearly the difference between actual and average tension and points out especially the sudden increase in tension

at the critical moment when the carrier reverses its movement as it comes near the braiding point.

Figure 29 shows the tendency of the thread tension to depend upon the position of the carrier eyelet or in relationship to the travel of the thread tension eyelet.

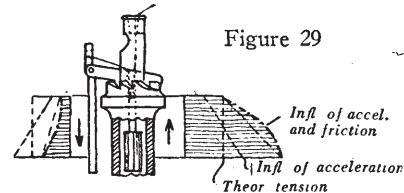


Figure 29

(b) Carrier with Tension Spring

In Figure 30 we find registered the curve for the travel of the *ideal* thread tension as taken from Figure 14\*—marked with a dotted

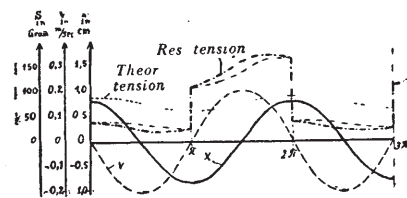


Figure 30

line—in its relationship to the curve of travel and speed. Assuming the speed equals 0 (for a very slow carrier movement) the momentary value of this ideal tension is multiplied by  $\mu$  higher = 1.83 and  $\mu$  lower = 0.44, and the thread tension thus found has been registered as the thin dash-dot line. This curve is correct for the two moments 0,  $\pi$ , and  $2\pi$ , because here the speed is 0 in actual fact. For all points between, however, the factor of friction  $\mu$  (as also shown previously in Figure 27) has to be taken into consideration for the different speeds as shown in Figure 26 and then the actual tension curve for each moment must be fixed. This curve of actual tension has been drawn in as a stronger dot-dash line. Figure 31 shows according to the same principle as applied in Figure 28, the ideal tension and the actual tension in polar coordinates and thus gives the dependency upon the momentary position of the carrier in its course. Finally,

\* See January issue, p. 1502.



in Figure 32, the curve of the thread tension is reproduced in its dependency upon the position of the tension eyelet of the carrier.

A comparison between the spring tension carrier (Figures 30 to 32) with the tension weight carrier (Figures 27 to 29) shows that

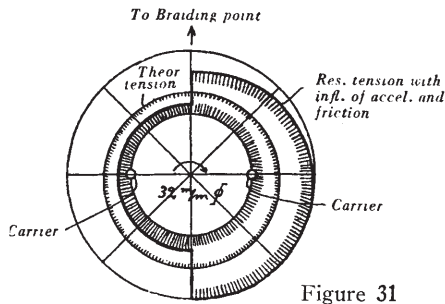


Figure 31

the sudden increase in thread tension on the spring tension carrier is less than half of the curve of the weight carrier. The total increase of thread tension on the spring carrier occurs in two steps and the second higher step is mounting comparatively slowly; the decrease in tension, however, is much more sudden.

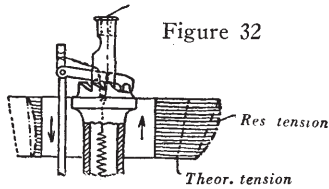


Figure 32

The illustrations point out the fact that under equal conditions the spring tension is much more favorable for the thread than the weight tension; this becomes especially evident for machines running at a higher rotating speed.

## VI. The Influence of Periodic Stopping and Starting Upon the Thread Tension

As mentioned before\* on the one thread lace machine carriers cannot twist continuously on the same plate, but the Jacquard mechanism is steering the yarn carrier in such a manner that after each half-turn of a driving plate (or quoit) a stop of the same duration has to occur. This stopping is effected each time at the exact moment when one carrier is at the point of leaving the working plate to slide

over to the neighboring plate. The diagrams shown in Figures 14 and 30, therefore, must be corrected for the special case of the one thread lace machine by inserting a rest period after the angular positions  $\pi/2$  and  $3/2\pi$ .

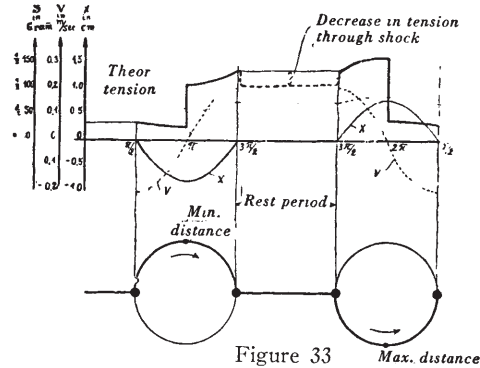


Figure 33

Figure 33 shows such a diagram for a one thread lace machine. The stopping and starting according to this sketch occurs at the time  $\pi/2$  at the moment when the thread tension has its lowest value or at the time  $3\pi/2$ , when the tension is halfway on its last increase. In both cases the thread tension eyelet has its moment of highest speed as is seen from the curve drawn into the sketch.

On account of the jerking stop of the carrier from full speed the thread tension, after reaching position  $3\pi/2$  will not keep its high value of 1.88 in regards to the ideal tension, but between both tensions there is a tendency of levelling. The levelling will be more evident with an intensive shock, or, expressed differently; higher working speed of the carrier at the moment of stopping results in a levelling of both curves.

Assuming the decrease in tension to occur about halfway between maximum tension and average tension this line is shown in Figure 33 accordingly. The actual position of the rest tension will be found according to later experiments depending upon the working speed of the machine. Logically, after stopping between the moments  $\pi/2$ , where the tension caused by friction is diminished, the actual thread tension under the influence of the shock has the tendency to equal the average tension. Since the difference in tension in this position is not considerable, any changes in thread tension are hardly noticeable.

(To Be Continued)

\* See THE MELLIAND, I, No. 5, page 706.

In the following table the values for  $\mu$  are:

$$\begin{aligned} \mu \text{ upward} &= \mu_1 \cdot \mu_2 \\ \mu \text{ downward} &= \frac{2 - \mu_1}{\mu_2} \end{aligned}$$

These values are considered in their dependency upon the speed of the thread passing through the tension eyelet  $a$ . On account of the block and pulley principle involved here the speed is only one half of the speed in the upper thread eyelet  $b$ , which must be considered when reading the values  $\mu_1$  and  $\mu_2$  and multiplying these to the product  $\mu_1 \cdot \mu_2$ .

In Figure 26 all curves belonging to the equations above mentioned are graphically shown.

$v$	$\mu_2$	$v/2$	$\mu_1$	$\mu_1 \cdot \mu_2$	$\frac{2 - \mu_1}{\mu_2}$
0	1.31	0	1.4	1.803	0.458
0.119	1.44	0.06	1.45	2.09	0.354
0.2	1.5	0.1	1.48	2.22	0.32
0.56	1.6	0.28	1.53	2.45	0.28
0.88	1.61	0.44	1.543	2.485	0.27
Comparison with test according to IV b					
0.051	1.37	0.025	1.433	1.96	0.413

According to Figures 12 to 14, the speed of the thread tension device runs harmoniously between 0 and 0.202 m/sec., at the same time the friction factor  $\mu$  at each turn of the horngear runs correspondingly according to the stronger marked part of the curves in

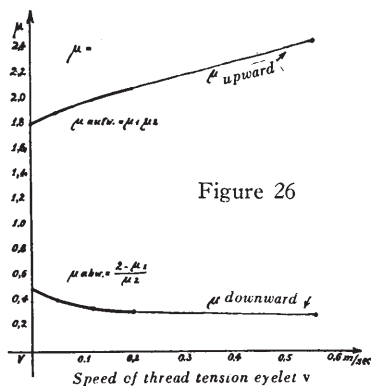


Figure 26. During the carrier movement away from the braiding point the upper curve is valid, during the period of carrier approach to the braiding point the lower curve is to be

accepted. By means of these curves we can fix the influence of friction for each moment of carrier movement. Accordingly we have the assurance to consider not only the acceleration but also the friction upon the curve of the thread tension shown in Figures 13 and 14. In the following chapter this will be taken into consideration.

## V. Course of Thread Tension Under Consideration of Forces of Acceleration and Friction

### (a) Carrier With Tension Weight.

Figure 27 shows the diagram of travel-time-speed with consideration of thread tension taken from Figure 13 influenced by acceleration. This influence is marked by a thin dotted line. For each point of the tension curve the corresponding speed may be taken from the V curve, also drawn in, and then we may read from Figure 26 the adequate value of  $\mu$  for this speed. Let us presume at first that the friction factor  $\mu$  is independent of speed and is equal to the value for speed = 0, taken from Figure 26; so we find

$$\mu \text{ upward} = 1.83$$

$$\mu \text{ downward} = 0.44$$

During the sliding down motion of the thread eyelet, this means during the time from 0 to  $\pi$ , the thread tension is diminished to the amount of 0.44; while during the time from  $\pi$  to  $2\pi$  the tension is increased to the amount of 1.83 for each momentary value. The curve thus found has been drawn in with a thin dot-dash line. This curve is correct for the moments

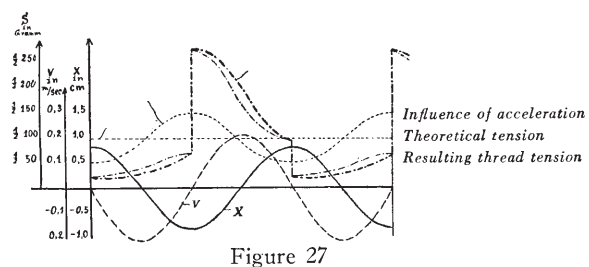


Figure 27. 0,  $\pi$  and  $2\pi$ , since here the speed curve actually crosses the zero sign; for the intermediate points we must yet consider the change of  $\mu$  caused by the influence of speed. For this purpose we may read off the speed from Fig-